Dihedral-angle-averaged Bethe lattice for vibrations in glasses

R. A. Barrio
Instituto de Investigaciones en Materiales, Universidad Nacional Autónoma de México (UNAM), Apartado Postal 70-360, 04510 México, Distrito Federal, México

F. L. Galeener
Xerox Corporation, Palo Alto Research Center, 3333 Coyote Hill Road, Palo Alto, California 94304 and Cavendish Laboratory, University of Cambridge, Madingley Road, Cambridge CB3 0HE, United Kingdom

E. Martinez
Departamento de Fisica Fundamental, Universidad Autónoma de Madrid, Canto Blanco, Madrid 34, Spain
(Received 8 January 1985)

An exact solution is found for a Bethe-lattice model of the vibrations in AX_2 glasses when the dihedral angle is assumed to be completely random and is averaged throughout the lattice. The vibrational density of states agrees very well with that calculated by Bell and co-workers for a large ball-and-stick model, and is much simpler to compute. The Raman, infrared, and inelastic neutron scattering spectra are calculated for vitreous SiO_2 and GeO_2, which show satisfactory agreement with the main features of the experimental spectra.

I. INTRODUCTION

There is much interest in understanding the structure and properties of glasses using dynamical probes that yield information about their vibrational modes. These probes are principally infrared, neutron, and Raman scattering. As a result, there is substantial experimental data, particularly on chalcogenide glasses[1] and silica,[2] that have not been fully exploited due to the difficulty of appropriate theoretical treatment.

Among the several theoretical approaches to the problem, we note the extensive calculations of Bell, Dean, and co-workers[3] and the analytical models based on the Bethe lattice.[4–6] Also of interest is the simpler central-forces-only theory by Sen and Thorpe[7] that, in spite of its simplicity, has been very useful in interpreting the polarized Raman spectra of these glasses.[8] Unfortunately, the central-forces-only theory does not always suffice because noncentral forces are frequently important, especially at lower frequencies, or in the case of intermediate-range order.

The introduction of noncentral forces in a Bethe-lattice calculation is not trivial because the relative positions of second neighbors is not known from experiment. Nevertheless, former Bethe-lattice calculations including noncentral forces[5,6] have been carried out assuming a particular configuration of atoms, an approximation that is unlikely to be justified in a glass.

In a previous paper[9] we have reported an efficient method to solve analytically the AX_2 Bethe lattice without having to impose a given configuration between second neighbors. It is the purpose of this paper to discuss that theory in detail and to compare the results with experimental data.

II. THEORY

The local arrangement of atoms in an AX_2 glass is shown in Fig. 1, where it is seen that two tetrahedral AX_4 units always share a corner (not edges, etc.). The relative positions of the two tetrahedra are defined by the "intertetrahedral" angle θ and the "dihedral" angle ϕ, measured in a frame of reference centered on one A atom whose polar axis is on the direction of one of the four tetrahedral bonds.

Let us consider a Born Hamiltonian, where the potential between two neighboring sites l and l', when there are small displacements $\mathbf{u}$ from the equilibrium positions, can be written

$$V_{ll'}=\tfrac{1}{2}(\alpha-\beta)\{[\mathbf{u}(l)-\mathbf{u}(l')]\cdot\hat{\mathbf{n}}_{ll'}\}^2 + \tfrac{1}{2}\beta[\mathbf{u}(l)-\mathbf{u}(l')]^2 , \quad (1)$$

where there is a central force of strength α acting along the unit vector joining the sites $\hat{\mathbf{n}}_{ll'}$, and a noncentral force

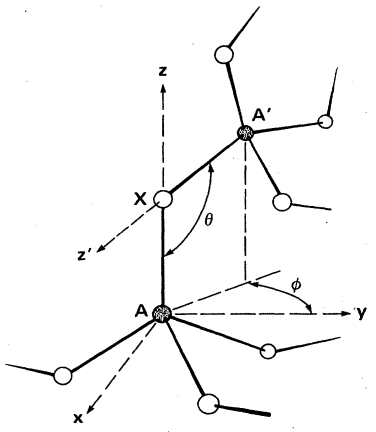

FIG. 1. Local geometry of two tetrahedral units in an AX_2 glass. The relative position of the frames of reference centered at A and A' is measured by the "intertetrahedral" angle θ, between the polar axes z and z', and by the "dihedral" angle ϕ.

β perpendicular to it.

The equations of motion for the Green's function[10] are

$$M_\mu(l')\omega^2 G_{\mu\mu'}(l,l';\omega) = \delta_{\mu\mu'}\delta(l,l') + \sum_{\mu''}\sum_{l''} D_{\mu\mu''}(l,l'')G_{\mu''\mu'}(l'',l';\omega) , \tag{2}$$

where $\underline{D}$ is the dynamical matrix, whose elements contain the second derivatives of (1) with respect to the various Cartesian components μ of the displacements, that is,

$$D_{\mu\mu'}(l,l') = \frac{\partial^2 V_{ll'}}{\partial u_\mu(l)\partial_{\mu'}(l')} .$$

Direct application of Eq. (2) to the present case poses a serious geometrical problem, because of the need to specify the exact position of each atom in the same frame of reference, and the set the equations rapidly becomes untractable. For this reason it is most convenient to define a different frame of reference centered at each A atom, in such a way that its four X neighbors are described in the same way everywhere. For instance, in Fig. 1 we show that the frames centered on A and A' both have a bond along their respective polar axes z and z'.

Therefore, we need a notation for the Green's function that states explicitly the kind of atom at each site, and the different frame of reference used; for example, let us write

$$\underline{G}^{AX'}(l,l') = \langle\langle \mathbf{u}^A(l);\mathbf{u}^{X'}(l');\omega \rangle\rangle , \tag{3}$$

where the angular brackets represent a quantum and a thermodynamical average[11] over the sample. This quantity is a 3×3 matrix that correlates the displacement of an atom of type A at site l with the displacement of an atom of type X at site l'. The prime on the X in (3) means that the corresponding $\mathbf{u}^X$ is written in a frame of reference different from the one used to describe $\mathbf{u}^A$.

Let us follow the nomenclature depicted in Fig. 2. The equation of motion for the atom of mass M labeled "origin" is then

$$\left[M\omega^2\underline{I} + \sum_{i=1}^{4}\underline{D}_i\right]\underline{G}^{AA}(0,0) = \underline{I} + \sum_{j=1}^{4}\underline{D}_j\underline{G}^{AX}(0,i) , \tag{4}$$

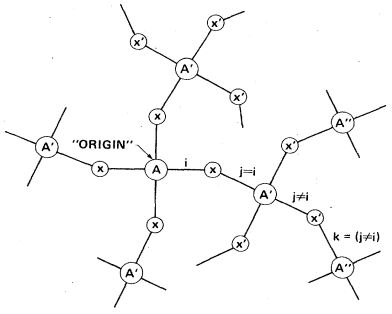

FIG. 2. Diagram showing the labeling of bonds used in the equations of motion. The atom labeled "origin" is at site 0 and subsequent sites are named after the bond arriving to them. Sites with the same number of primes are referred to the same frame of reference.

where $\underline{I}$ is the identity matrix and $\underline{D}_i$ is the interaction matrix between the A-X pair along one of the tetrahedral directions, $i=1,2,3,4$. For instance, if the z axis coincides with direction 1, it is clear that

$$\underline{D}_1 = \begin{bmatrix} -\beta & 0 & 0 \\ 0 & -\beta & 0 \\ 0 & 0 & -\alpha \end{bmatrix} , \tag{5}$$

Also, the matrices $\underline{D}$ are related by the tetrahedral symmetry

$$\sum_{i=1}^{4}\underline{D}_i = -\tfrac{4}{3}(\alpha+2\beta)\underline{I} . \tag{6}$$

Along the direction i we have

$$(m\omega^2\underline{I} + \underline{D}_i + \underline{R}_i^{-1}\underline{D}_i\underline{R}_i)\underline{G}^{AX}(0,i) = \underline{D}_i\underline{G}^{AA}(0,0) + \underline{R}_i^{-1}\underline{D}_i\underline{G}^{AA'}(0,i) , \tag{7}$$

where m is the mass of the atom X.

Notice that the vectors in the last term in (7) are described in different frames. A vector defined in the frame centered at A' is transformed to the original frame according to $\underline{R}_i^{-1}\mathbf{v}'=\mathbf{v}$. From Fig. 1 it is clear that $\underline{R}_i = \underline{\Theta}_i\underline{\Phi}_i$, where $\underline{\Phi}_i$ is a rotation of ϕ degrees around axis $\hat{\mathbf{n}}_{0i}$ and $\underline{\Theta}_i$ is a rotation by $\pi-\theta$ around an axis perpendicular to it, specifically,

$$\underline{\Phi}_i = \begin{bmatrix} \cos\phi_i & \sin\phi_i & 0 \\ -\sin\phi_i & \cos\phi_i & 0 \\ 0 & 0 & 1 \end{bmatrix}$$

and

$$\underline{\Theta}_i = \begin{bmatrix} 1 & 0 & 0 \\ 0 & -\cos\theta_i & \sin\theta_i \\ 0 & -\sin\theta_i & -\cos\theta_i \end{bmatrix} .$$

It must be clear that

$$\left[M\omega^2\underline{I} + \sum_{l=1}^{4}\underline{D}_l\right]\underline{G}^{AA'}(0,i) = \underline{D}_i\underline{R}_i\underline{G}^{AX}(0,i) + \sum_{j\neq i}\underline{D}_j\underline{G}^{AX'}(0,j) . \tag{8}$$

Let us use a shorthand notation:

$$\underline{A}_i = \underline{A}_i(\theta_i,\phi_i) = m\omega^2\underline{I} + \underline{D}_i + \underline{R}_i^{-1}(\theta_i,\phi_i)\underline{D}_i\underline{R}_i(\theta_i,\phi_i) . \tag{9}$$

We need a further equation

$$\underline{A}_j\underline{G}^{AX'}(0,j) = \underline{D}_j\underline{G}^{AA'}(0,i) + \underline{R}_j^{-1}\underline{D}_j\underline{G}^{AA''}(0,j) . \tag{10}$$

Now Eqs. (4), (7), (8), and (10) from a complete set that can be solved in the Bethe lattice by defining the follow-

ing transfer matrices:

$$\underline{G}^{AA'}(0,i)=\underline{T}_i\underline{G}^{AA}(0,0) \tag{11}$$

and

$$\underline{G}^{AA''}(0,j)=\underline{T}_j\underline{G}^{AA'}(0,i)\ . \tag{12}$$

Substitution into the proper equations of motion gives an equation for $\underline{T}_i$:

$$\underline{T}_i=\left[M\omega^2\underline{I}+(\underline{D}_i-\underline{D}_i\underline{R}_i\underline{A}_i^{-1}\underline{R}_i^{-1}\underline{D}_i)+\sum_{j\neq 1}(\underline{D}_j-\underline{D}_j\underline{A}_j^{-1}\underline{D}_j-\underline{D}_j\underline{A}_j^{-1}\underline{R}_j^{-1}\underline{D}_j\underline{T}_j)\right]^{-1}\underline{D}_i\underline{R}_i\underline{A}_i^{-1}\underline{D}_i\ , \tag{13}$$

whose solution can be put into (4) to give

$$\underline{G}^{AA}(0,0)=\left[M\omega^2\underline{I}-\sum_{i=1}^{4}\underline{K}_i\right]^{-1}, \tag{14}$$

which defines a self-energy $\underline{K}_i$ due to the mechanical impedance attached to each bond i. It is clear that

$$\underline{K}_i=-\underline{D}_i+\underline{D}_i\underline{A}_i^{-1}\underline{D}_i+\underline{D}_i^{\text{eff}}\underline{T}_i\ , \tag{15}$$

where

$$\underline{D}_i^{\text{eff}}=\underline{D}_i\underline{A}_i^{-1}\underline{R}_i^{-1}\underline{D}_i\ .$$

The actual solution of (13) requires the exact specification of all the matrices in the infinite set $\{\underline{R}_i\}$. This is impossible if the angles θ_i and ϕ_i vary from site to site. Therefore, it is necessary to introduce some approximations at this point:

(1) Let us assume that θ is the same for any A-X-A unit. This is reasonable since the dispersion of θ in SiO_2 reported from x-ray studies,[12] or from hand-built models,[13] is small ($\pm 10\%$). Nevertheless, we will investigate the effects of introducing disorder in θ in the next section.

(2) The dihedral angles ϕ_i are completely random in the glass. This assumption holds if there is no evidence of intermediate-range order in the network, and it means that the value of ϕ in a particular place in the lattice does not depend on the values of ϕ elsewhere. There is evidence[14] that geometrical constraints introduce strong correlation between ϕ's associated with neighbor bonds, but even so, the mean distribution of ϕ is reasonably flat. This latter approximation allows one to perform an average of Eq. (14) in the spirit of the random-phase approximation.[10] Then

$$\langle\underline{G}^{AA}(0,0)\rangle=\underline{G}=\left[M\omega^2\underline{I}-\sum_{i=1}^{4}\langle\underline{K}_i\rangle\right]^{-1}, \tag{16}$$

where $\langle\ \rangle$ stands for an unweighted averaged over ϕ. This allows one to solve the Bethe lattice exactly. The averaged self-energy per bond is

$$\langle\underline{K}_i\rangle=-\underline{D}_i+\underline{D}_i\langle\underline{A}_i^{-1}\rangle\underline{D}_i+\langle\underline{D}_i^{\text{eff}}\underline{T}_i\rangle\ . \tag{17}$$

The calculation of $\langle\underline{K}_i\rangle$ is straightforward and is given in Appendix A. It is seen that all quantities of interest can be written in terms of $\langle\underline{K}_i\rangle$, for instance, $\underline{G}$ is obtained with (16) using (6). As a further example, let us calculate the autocorrelations on a site X. For bond 1 the appropriate equations of motion are

$$\underline{A}_1(\theta,0)\underline{G}^{XX}(1,1)=\underline{I}+\underline{D}_1\underline{G}^{XA}(1,0)+\underline{R}_1^{-1}\underline{D}_1\underline{G}^{XA'}(1,1)\ , \tag{18}$$

$$\underline{Z}_1\underline{G}^{XA}(1,0)=\underline{D}_1\underline{G}^{XX}(1,1)\ , \tag{19}$$

$$\underline{Z}_1\underline{G}^{XA'}(1,1)=\underline{D}_1\underline{R}_1\underline{G}^{XX}(1,1)\ , \tag{20}$$

where

$$\underline{Z}_1=M\omega^2\underline{I}+\underline{D}_1-\sum_{j\neq 1}\underline{K}_j\ . \tag{21}$$

The averaged Green's function $\langle\underline{G}^{XX}(1,1)\rangle$ is diagonal in the representation introduced by Bell, Dean, and Hibbins-Butler,[15] $(x,y,z)=(R,B,S)$, in which the A-X-A plane is perpendicular to the $x=R$ axis and the $y=B$ axis bisects the angle θ. This latter representation differs from the one we have used by a rotation $\underline{\psi}$ around the x axis by $(\pi-\theta)/2$. Let us call

$$\underline{g}=\underline{\psi}^{-1}\langle\underline{G}^{XX}(1,1)\rangle\underline{\psi}\ , \tag{22}$$

then, the elements of $\underline{g}$ are

$$g^R=\{m\omega^2-2\epsilon\}^{-1}\ , \tag{23a}$$

$$g^B=\{m\omega^2-2[\epsilon\sin^2(\phi/2)+\lambda\cos^2(\theta/2)]\}^{-1}\ , \tag{23b}$$

$$g^S=\{m\omega^2-2[\epsilon\cos^2(\theta/2)+\lambda\sin^2(\theta/2)]\}^{-1}\ , \tag{23c}$$

where

$$\epsilon=\beta+\beta^2/[M\omega^2-\beta-(4\langle K_{\parallel}\rangle+5\langle K_{\perp}\rangle)/3]\ ,$$

$$\lambda=\alpha+\alpha^2[M\omega^2-\alpha-(\langle K_{\parallel}\rangle+8\langle K_{\perp}\rangle)/3]\ .$$

It is clear that correlations between neighbors $\langle\underline{G}^{AX}(1,0)\rangle$ are immediately obtained from (19).

III. DENSITY OF STATES

In this section we will illustrate the kind of results obtained with the present theory by examining the vibrational density of states (DOS), which is given, per AX_2 unit, by

$$\rho(\omega)=\frac{-2\omega}{3\pi}\text{Im}(M\ \text{Tr}\underline{G}+2m\ \text{Tr}\underline{g})\ , \tag{24}$$

where $\underline{G}$ and $\underline{g}$ are given by (16) and (22), respectively. One can also investigate the contribution of certain modes to the DOS, for instance

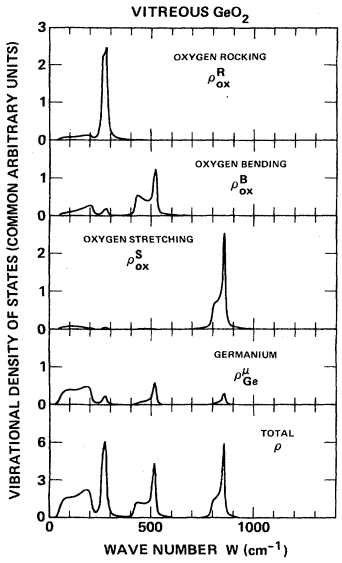

FIG. 3. Theoretical densities of states for GeO_2. Notice that there are three well-separated bands for the oxygen motion. An imaginary part of $\sim 5\ cm^{-1}$ was added to the frequency.

$$\rho_x^\gamma(\omega)=\frac{-2m\omega}{\pi}\mathrm{Im}g^\gamma,\quad \gamma=R,B,S \tag{25a}$$

is the partial density on site X and direction γ, and

$$\rho_A^\mu(\omega)=\frac{-2M\omega}{\pi}\mathrm{Im}G,\quad \mu=x,y,z \tag{25b}$$

is the partial density of a tetrahedral site A, which is isotropic. In Figs. 3 and 4 we show the results from (24) and (25) for parameters appropriate to GeO_2 and SiO_2, respectively. The parameters were chosen to best fit the broad features of the experimental spectra and their values are given in Table I. It is worthwhile to note that these values are in close agreement with the ones obtained by other methods,[16] particularly the angle θ for SiO_2 which is quite near the value 152° obtained by the latest x-ray measurements.[17]

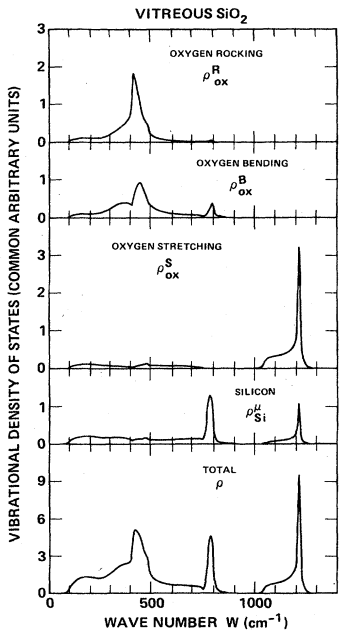

FIG. 4. Same as Fig. 3 for SiO_2. Notice that the rocking and bending bands overlap in the lower half of the spectrum.

TABLE I. Parameters used for GeO_2 and SiO_2.

	α (N/m)	β (N/m)	θ (degree)
GeO_2	341	31	133
SiO_2	507	78	154

There is one important difference between these glasses. We notice that the oxygen bands are well separated in GeO_2, but they strongly overlap in SiO_2, particularly the rocking and bending bands. This fact accounts for the main differences in the Raman spectra of these glasses, as we shall see in the next section.

In order to see how good our results are, we compare them with others already available. Among them there are the very well documented calculations for a ball-and-stick model by Bell, Bird, and Dean[18] (BBD). The BBD calculation is one of the most realistic performed to date. Figure 5(a) shows our results for GeO_2 calculated with the parameters reported in BBD and averaged over several angles θ, with a triangular distribution centered at 140°,

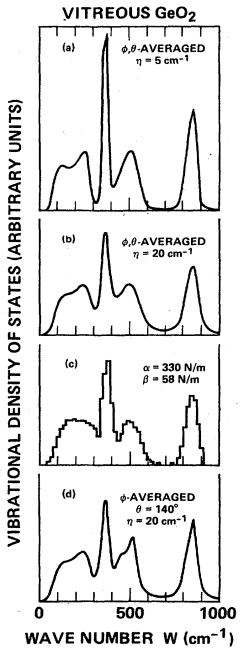

FIG. 5. Comparison of the density of states for GeO_2 obtained with the present theory and results from numerical calculations in a hand-built model. (a) Averaged over a flat distribution of ϕ and a triangular distribution of θ. (b) Same as (a) but with a large imaginary part (η) added to the frequency. (c) Histogram obtained by BBD (Ref. 18). (d) Theoretical result with a fixed value of θ. Notice that panels (b) and (c) are practically identical.

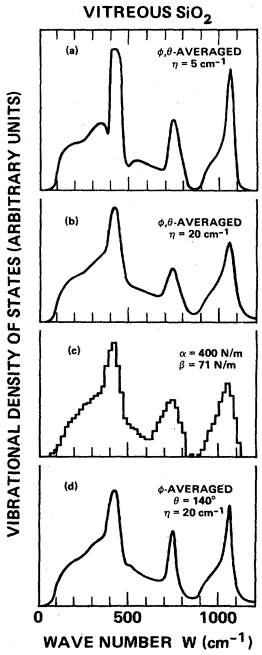

FIG. 6. Same as Fig. 5 for SiO_2. Here the comparison between panels (b) and (d) shows that the main effect of the disorder in θ is to broaden the oxygen-bending band at ~ 750 cm^{-1}.

which resembles the actual distribution on the physical model reported by Bell and Dean.[13] The BBD calculation is shown in Fig. 5(c), and as we compare it with ours we notice that our bands are too narrow, as expected from a Bethe-lattice model. However, if we artificially broaden the spectrum by introducing a reasonably large imaginary part to the frequency ($\eta = 20$ cm^{-1}), as in Fig. 5(b), our spectrum becomes practically identical with the one by BBD [Fig. 5(c)]. The broadening can be justified by considering that we did not allow for distortions of the tetrahedra that were certainly present in the hand-built model, and whose effect would be to broaden the bands.

Figure 5(d) shows the broadened DOS for a single value of θ. One can see that the effect of the disorder in θ is not important, as far as the DOS is concerned, and its main effect is to broaden the peaks slightly, particularly the oxygen-bending band. Therefore, one can conclude that keeping a fixed θ is not an unreasonable approximation while working with this theory.

The same comparisons are presented for SiO_2 in Fig. 6. We notice that for this glass the resemblance of panels *b* and *c* is even more striking, and that the effect of disorder in θ is somewhat more noticeable.

IV. SCATTERING RESPONSES

The DOS is related to measurable intensities in scattering experiments through the Fermi "golden rule," although the DOS is not directly comparable with the experiment because of unknown matrix-element effects, which may produce substantial differences between the spectra and the DOS. In this section we discuss approximate ways of calculating scattering intensities from the correlations already found.

A. Polarized Raman scattering

The Raman polarizability is proportional to[19]

$$\frac{-2\omega f(\omega)}{\pi} \sum_{l,l'} (\nabla\alpha_l)\cdot \mathrm{Im}\underline{G}(l,l')\cdot(\nabla\alpha_{l'}) , \tag{26}$$

where α_l is the polarizability associated with atom l, and $f(\omega)$ is a slowly varying function of ω. Martin and Galeener[20] have obtained an approximate expression for $\nabla\alpha_{l'}$ based on a model of Alben *et al.*[21] They show that the polarized part of the Raman spectrum can be calculated from

$$\mathrm{Im}\left[\sum_{\mu,\nu}\sum_{l,l'} \bar{v}^{\,l}_{\mu} G_{\mu\nu}(l,l')\bar{v}^{\,l'}_{\nu}\right] , \tag{27}$$

where

$$\bar{v}^{\,l} = \sum_{m} \hat{\mathbf{n}}_{lm} .$$

Here the summation runs over all the m bonds arriving at site l, and $\hat{\mathbf{n}}_{lm}$ is a unit vector along a given bond.

The summation in (27) involves correlations between all sites, and it is possible to perform such an infinite summation in the Bethe lattice.[22] However, this procedure leads to unphysical results (for details see Yndurain *et al.*[23]). Therefore, we decided to neglect long-range correlations, in fact we calculated (27) by taking into account only the eight bonds associated with a five-atom cluster. We calculated this using the cluster Bethe-lattice method,[24] that is, we treated the dynamics of a five-atom cluster exactly and attached Bethe lattices to the free bonds. The full Green's function is now a 15×15 matrix that is explicitly shown in Appendix B.

Notice that $\bar{v}^{\,l}=0$ for sites with tetrahedral symmetry; therefore, only the oxygen sites contribute to the Raman intensity. The results are shown in Fig. 7 for GeO_2 and in

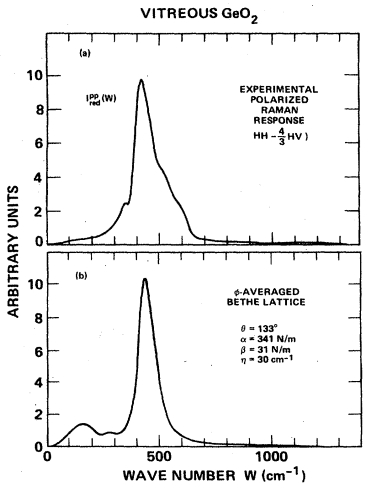

FIG. 7. Comparison between the experimental (a) and theoretical (b) polarized Raman spectra of GeO_2. The experimental curve is from Ref. 27.

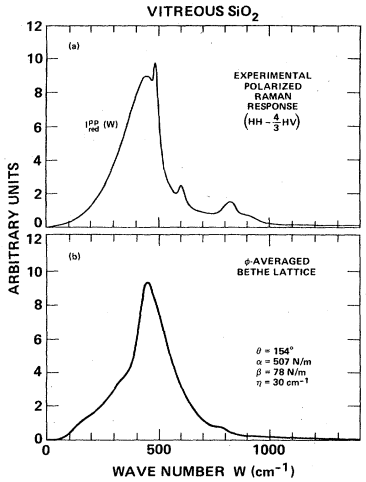

FIG. 8. Same as Fig. 7 for SiO_2. The sharp peaks in (a) are not reproduced in (b) because they arise from defects in the glass structure (Ref. 26).

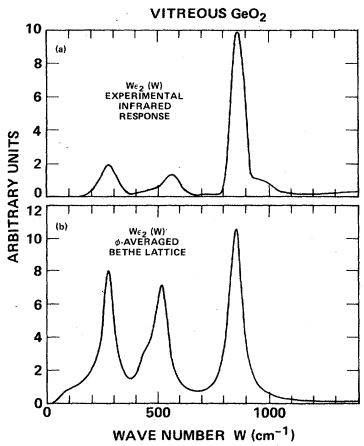

FIG. 9. (a) Experimental infrared response of GeO_2 and (b) calculated with the present theory assuming fixed-point charges on each site.

Fig. 8 for SiO_2.

The comparison with actual experiments shows that the theory reproduces the main features very well: the number of peaks, their relative intensity, and weights. This tends to justify our truncation in (27) and suggests that in the real glasses the disorder "screens" correlations between distant sites.

The sharp peaks shown in the spectra are not reproduced by the theory since they arise from defects not introduced in the model. At present, there is substantial discussion concerning the nature of such defects,[25] although there is strong evidence that they are regular low-member rings.[26] It is not hard to imagine that the present theory is suitable for the study of local defects in a random network. A detailed analysis of defects and rings in glasses is in preparation and will be published soon.

B. Infrared absorption

Another quantity that can be derived from the displacement-displacement Green's function is the phonon contribution to the complex dielectric function ($\epsilon=\epsilon_1+i\epsilon_2$):

$$\epsilon=1+\frac{4\pi}{V}\mathrm{Tr}\left[\sum_{l,l'} e(l)G(l,l')e(l')\right],$$

where V is the volume of the sample and $e(l)$ is the dynamical effective charge tensor, whose elements are the derivatives of the dipole moment associated with a site with respect to the displacements. Galeener *et al.*[27] have examined in detail the measurable reflectivity at normal incidence in an experiment and its relation with

$$\omega\epsilon_2 \sim \omega\,\mathrm{Im}\,\mathrm{Tr}\left[\sum_{l,l'} e(l)G(l,l')e(l')\right]. \quad (28)$$

We calculated this equation using the same cluster, given in Appendix B, and performing the same average over the 256 configurations. We approximated the charge tensors by fixed-point charges $+4$ at the Si site and -2 at each oxygen site.

In Fig. 9 we show the infrared spectrum of GeO_2 compared with experiment. We notice that the correct number of active modes are placed at the right frequencies. However, the relative intensity of the peaks is not very satisfactory.

In order to investigate the effect of the approximations involved, we calculated Eq. (28) from a nine-atom cluster and the result did not improve. Therefore, we must conclude that the discrepancy in intensities is due to the fixed-charge approximation, which does not allow for the fact that there is charge transfer between nearest neighbors during the motion (due to a change in the bond energy with distance between sites). We also performed a calculation using a method similar to the one given by Harrison,[28] but this did not improve either of the results. It is clear that three different parameters for the components of the dynamical charge could be fitted to give the observed intensities of the three peaks. But no further insight is gained by doing this; therefore, we have not car-

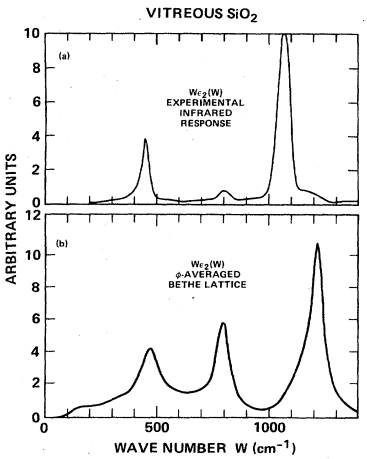

FIG. 10. Same as Fig. 9 for SiO_2. The very intense response of the oxygen-bending band is due to the fixed-charge approximation.

ried out the procedure.

Figure 10 shows the same comparison for SiO_2; here, the comparatively large response of the bending mode is even more noticeable. The high-frequency peak is not placed correctly because of difficulties with the large LO-TO splitting of the modes in that region,[29] that obviously can not be obtained with the present theory.

C. Inelastic neutron scattering

The measurable quantity in a neutron scattering experiments is

$$N(q,\omega)=\frac{\mathbf{K}_0}{\mathbf{K}}\frac{2\omega}{q^2[n(\omega)+1]}\frac{\partial^2\sigma}{\partial\Omega\,\partial\omega}\ ,$$

where $\mathbf{q}=\mathbf{K}-\mathbf{K}_0$ is the difference between the scattered and incident wave vectors, and $n(\omega)$ is the phonon population at a given temperature. The incoherent part of the scattering is closely related to the DOS: it is shown[30] that the differential cross section is

$$\frac{\partial^2\sigma}{\partial\Omega\,\partial\omega}=\frac{-\mathbf{K}}{\pi 3\mathbf{K}_0}q^2\sum_{\mu,l}[a_\mu^{\rm inc}(l)]^2{\rm Im}G_{\mu\mu}(l,l)\ ,$$

where $[a_\mu(\omega)]$ includes the Debye-Waller factor and the scattering lengths. Then the "reduced" intensity is

$$[n(\omega)+1]N^{\rm inc}=N=\sum_{\mu,l}[a_\mu(l)]^2\frac{2\omega}{3\pi}{\rm Im}G_{\mu\mu}(l,l)\ ,$$

which is the case of AX_2 glasses reduces to

$$N=\sum_\mu\left[\frac{[a_\mu(A)]^2}{M}\rho_A^\mu+\frac{2[a_\mu(x)]^2}{m}\rho_x^\mu\right]. \tag{29}$$

In Figs. 11 and 12 we show the neutron intensities obtained from (29) using the scattering lengths reported in Ref. 31. The absence of the double peak at high frequencies due to the LO-TO splitting is more noticeable in this case, although the overall shape of the spectrum is reproduced with remarkable accuracy, particularly the SiO_2 spectrum.

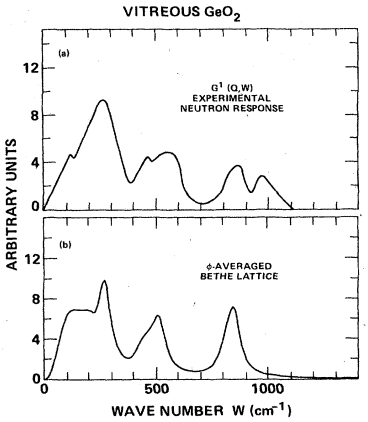

FIG. 11. (a) Reduced one-phonon neutron response $G(Q,\omega)$ for GeO_2 fom Ref 27. (b) Theoretical incoherent neutron spectrum from Eq. (29).

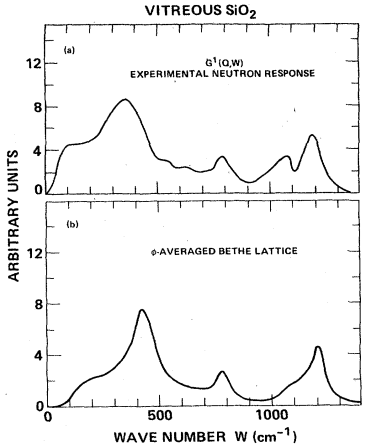

FIG. 12. Same as Fig. 11 for SiO_2. The double-peak structure is not reproduced by the theory because it arises from a LO-TO splitting (Ref. 26).

V. CONCLUSIONS

We have reported a theory that enables one to calculate the displacement-displacement Green's function in a dihedral-angle-averaged Bethe lattice, suitable for AX_2 glasses. We have used it to calculate approximate spectra for vitreous SiO_2 and GeO_2 that compare well with the experimental data. The dihedral-angle-averaged Bethe lattice sheds new light on the nature of the vibrational modes in these materials and is a powerful tool for the study of local configurations, when used to represent the network attached to the local cluster. Such cluster calculations will help in vibrational studies of the intermediate-range order that can be present in these disordered solids. The simplicity of our theoretical results make the method efficient for use in more complex calculations. The results are readily adapted (or rederived) for application to other glasses having different topologies. The comparison made in Sec. III with the ball-and-stick model results illustrates the versatility of the method, since it proves that one need not build a new ball-and-stick model to deal with a new structure with similar accuracy. The comparison with experiment illustrates the ability of the "continuous-random-network" model to explain the broad features in the vibrational spectra of these materials.

ACKNOWLEDGMENTS

The authors are grateful for support of this work by the U.S. Office of Naval Research (through G.B. Wright). R.A.B. and E.M. wish to thank Xerox Palo Alto Research Center for its hospitality during their visits when much of this work was carried out.

APPENDIX A

In this section we will show in detail how to obtain the solution for the averaged self-energy $\langle \underline{K}_i \rangle$. It is sufficient to only consider $\langle \underline{K}_1 \rangle$, since the self-energies along

the other bonds are related by the tetrahedral symmetry [Eq. (6)].

Along bond 1, the expressions are simple:

$$\langle \underline{A}_1^{-1} \rangle = \begin{bmatrix} A_\perp^{-1} & 0 & 0 \\ 0 & A_\perp^{-1} & 0 \\ 0 & 0 & A_\parallel^{-1} \end{bmatrix}, \tag{A1}$$

where

$$A_\perp^{-1} = \frac{1}{k}\left[m\omega^2 - 2\alpha - (\beta-\alpha)\sin^2\theta + \frac{(\beta-\alpha)(m\omega^2-\alpha-\beta)\sin^2\theta}{2m\omega^2-4\beta} \right],$$

$$A_\parallel^{-1} = \frac{1}{k}[m\omega^2 - 2\beta + (\beta-\alpha)\sin^2\theta],$$

and

$$k = (m\omega^2-\alpha-\beta)^2 - (\beta-\alpha)^2\cos^2\theta .$$

After much algebraic manipulation one obtains

$$\langle \underline{D}_1^{\text{eff}} \underline{T}_1 \rangle = \langle \underline{\Phi}^{-1} \underline{H}^{-1} \underline{\Phi} \rangle = \begin{bmatrix} T_\perp & 0 & 0 \\ 0 & T_\perp & 0 \\ 0 & 0 & T_\parallel \end{bmatrix}, \tag{A2}$$

where

$$\underline{H} = \underline{D}_1^{-1} \underline{\Theta}^{-1} \underline{A}_1(-\theta,0)[\underline{D}_1^{-1} \underline{U} \underline{D}_1 \underline{A}_1(-\theta,0) - \underline{I}] \underline{\Theta} \underline{D}_1^{-1} . \tag{A3}$$

The matrix $\underline{U}$ is diagonal also, and its elements are

$$U_{11} = U_{22} = M\omega^2 - \tfrac{4}{3}(\alpha+2\beta) - \tfrac{1}{3}(4\alpha^2 A_\parallel^{-1} + 5\beta^2 A_\perp^{-1}) - \tfrac{1}{3}(4T_\parallel + 5T_\perp), \tag{A4}$$

$$U_{33} = M\omega^2 - \tfrac{4}{3}(\alpha+2\beta) - \tfrac{1}{3}(\alpha^2 A_\parallel^{-1} + 8\beta^2 A_\perp^{-1}) - \tfrac{1}{3}(T_\parallel + 8T_\perp), \tag{A5}$$

where we have used the property (6). The nonzero elements of $\underline{A}_1(-\theta,0)$ are

$$a_{11} = m\omega^2 - 2\beta ,$$
$$a_{22} = m\omega^2 - \beta(1+\cos^2\theta) - \alpha\sin^2\theta ,$$
$$a_{33} = m\omega^2 - \alpha(1+\cos^2\theta) - \beta\sin^2\theta ,$$
$$a_{23} = a_{32} = -(\beta-\alpha)\sin\theta\cos\theta .$$

Defining the quantities

$$a = a_{11}(U_{11}a_{11}/\beta^2 - 1) ,$$
$$b = a_{22}(U_{22}a_{22}/\beta^2 - 1) + U_{33}a_{23}^2/\alpha^2 ,$$
$$c = a_{33}(U_{33}a_{33}/\alpha^2 - 1) + U_{11}a_{23}^2/\beta^2 ,$$
$$d = a_{23}(U_{11}a_{22}/\beta^2 + U_{33}a_{33}/\alpha^2 - 1) ,$$

the nonzero elements of H can be written as

$$H_{11} = a/\beta^2 ,$$
$$H_{22} = \frac{1}{\beta^2}(b\cos^2\theta + c\sin^2\theta + 2d\sin\theta\cos\theta) ,$$
$$H_{33} = \frac{1}{\alpha^2}(b\sin^2\theta + c\cos^2\theta - 2d\sin\theta\cos\theta) ,$$
$$H_{23} = \frac{1}{\alpha\beta}[d\cos^2(2\theta) - (b-c)\sin\theta\cos\theta] .$$

Finally one obtains one set of scalar coupled linear equations for the transfer matrix

$$T_\perp = \frac{1}{2}\left[\frac{1}{H_{11}} + \frac{H_{33}}{H_{22}H_{33} - H_{23}^2} \right], \tag{A6a}$$

$$T_\parallel = \frac{H_{22}}{H_{22}H_{33} - H_{23}^2} , \tag{A6b}$$

which can be solved self-consistently to any degree of accuracy. Strictly speaking, Eqs. (A4), (A5), and (A6) can be combined to obtain a quartic equation for ω^2, and therefore the solution of (A6) can be obtained *analytically*. However, we think that an iterative solution of (A6) is very convenient, since we have seen that with this procedure, it always converges to the correct physical root.

We note that the solution (A6) reduces to the expression by Sen and Thorpe[7] in the case where $\beta=0$, and that it reproduces the results by Laughlin and Joannopoulos[5] when one suppresses the average and gives the appropriate fixed values to ϕ.

APPENDIX B

A five-atom cluster with Bethe lattices attached to the outer bonds ($i=1,2,3,4$) can be treated in closed form. Using the same notation as before, one can write the full Green's function for the cluster as follows:

$$\underline{G} = \begin{bmatrix} \left[M\omega^2\underline{I} + \sum_{i=1}^{4} \underline{D}_i \right] & -\underline{D}_1 & -\underline{D}_2 & -\underline{D}_3 & -\underline{D}_4 \\ -\underline{D}_1 & \underline{Q}_1 & 0 & 0 & 0 \\ -\underline{D}_2 & 0 & \underline{Q}_2 & 0 & 0 \\ -\underline{D}_3 & 0 & 0 & \underline{Q}_3 & 0 \\ -\underline{D}_4 & 0 & 0 & 0 & \underline{Q}_4 \end{bmatrix}^{-1}, \tag{B1}$$

where

$$\underline{Q}_i = \underline{\Phi}_i^{-1}[\underline{A}_i(-\theta,0) - \underline{\Theta}^{-1}\underline{D}_i\langle \underline{Z}_i^{-1} \rangle \underline{D}_i \underline{\Theta}] \underline{\Phi}_i . \tag{B2}$$

Each entry in (B1) is a 3×3 matrix. $\underline{\Theta}$ and $\underline{\Phi}_i$ are rotation matrices which account for the orientation of the cluster surface bonds. In evaluating (B1) we averaged over 256 different configurations with random ϕ_i's.

[1]R. Nemanich, *Proceedings of the Tenth International Conference on Amorphous and Liquid Semiconductors* [J. Non-Cryst Solids **59**, 851 (1984)].
[2]See, for instance, J. C. Phillips, Solid State Phys. **37**, 93 (1982).
[3]R. J. Bell, in *Excitations in Disordered Systems,* edited by M. F. Thorpe (Plenum, New York, 1981), p. 333.
[4]F. Yndurain and P. N. Sen, Phys. Rev. B **14**, 531 (1976).
[5]R. B. Laughlin and J. D. Joannopoulos, Phys. Rev. B **16**, 2942 (1977).
[6]C. Lucovsky, C. K. Wong, and W. B. Pollard, *Proceedings of the Tenth International Conference on Amorphous and Liquid Semiconductors* [J. Non-Cryst. Solids **59**, 839 (1984)].
[7]P. N. Sen and M. F. Thorpe, Phys. Rev. B **15**, 4030 (1977).
[8]F. L. Galeener, Phys. Rev. B **19**, 4292 (1979).
[9]R. A. Barrio, F. L. Galeener, and E. Martinez, Phys. Rev. Lett. **52**, 1786 (1984).
[10]R. J. Elliott, J. A. Krumhansl, and P. L. Leath, Rev. Mod. Phys. **46**, 465 (1974).
[11]D. N. Zubarev, Ups. Fiz. Nauk **71**, 71 (1960) [Sov. Phys.—Ups. **3**, 320 (1960)].
[12]R. L. Mozzi and B. E. Warren, J. Appl. Phys. **53**, 8615 (1982).
[13]R. J. Bell and P. Dean, Philos. Mag. **25**, 1381 (1972).
[14]F. L. Galeener (unpublished).
[15]R. J. Bell, P. Dean, and D. C. Hibbins-Butler, J. Phys. C **4**, 1214 (1971).
[16]F. L. Galeener, J. Phys. (Paris) Colloq. **42**, C6-24 (1981).
[17]J. R. G. Da Silva, D. G. Pinatti, C. E. Anderson, and M. L. Rudee, Philos. Mag. **31**, 713 (1975).
[18]R. J. Bell, N. F. Bird, and P. Dean, J. Phys. C **1**, 299 (1968).
[19]M. Cardona, in *Light Scattering in Solids II,* edited by M. Cardona and G. Güntherodt (Springer-Verlag, Berlin, 1982).
[20]R. Martin and F. L. Galeener, Phys. Rev. B **23**, 3871 (1981).
[21]R. Alben, D. Weaire, J. E. Smith, Jr., and M. H. Brodsky, Phys. Rev. B **11**, 2271 (1975).
[22]R. J. Elliott, R. A. Barrio, and M. F. Thorpe, KINAM **42**, 55 (1982).
[23]F. Yndurain, R. A. Barrio, R. J. Elliott, and M. F. Thorpe, Phys. Rev. B **28**, 3576 (1983).
[24]J. D. Joannopoulos and F. Yndurain, Phys. Rev. B **10**, 5164 (1974).
[25]J. C. Phillips. J. Non-Cryst. Solids **63**, 347 (1984).
[26]F. L. Galeener, Solid State Commun. **44**, 1037 (1982); J. Non-Cryst. Solids **49**, 53 (1982).
[27]F. L. Galeener, A. J. Leathbetter, and M. W. Stringfellow, Phys. Rev. B **27**, 1052 (1983).
[28]W. A. Harrison, *Electronic Structure and the Properties of Solids* (Freeman, San Francisco, 1980), p. 273.
[29]F. L. Galeener and G. Lucovsky, Phys. Rev. Lett. **37**, 1474 (1976).
[30]R. A. Barrio, R. J. Elliott, and M. F. Thorpe, J. Phys. C **16**, 3425 (1983).
[31]C. G. Windsor, *Pulsed Neutron Scattering* (Taylor and Francis, London, 1981), p. 407.